

Phytoplankton distribution and survival in the thermocline

Jonathan Sharples¹ and C. Mark Moore

Southampton Oceanography Centre, Empress Dock, Southampton, SO14 3ZH, United Kingdom

Tom P. Rippeth

School of Ocean Sciences, University of Wales, Bangor, Menai Bridge, Gwynedd, LL59 5EY, United Kingdom

Patrick M. Holligan and David J. Hydes

Southampton Oceanography Centre, Empress Dock, Southampton, SO14 3ZH, United Kingdom

Neil R. Fisher and John H. Simpson

School of Ocean Sciences, University of Wales, Bangor, Menai Bridge, Gwynedd, LL59 5EY, United Kingdom

Abstract

Observations of the vertical structure of density, concentrations of chlorophyll *a* and nitrate, and turbulent dissipation rates were made over a period of 25 h in a well-stratified shelf region in the Western English Channel, between neap and spring tides. Maximum turbulent dissipation at the base of the thermocline occurred almost 5 h after maximum tidal currents. This turbulence aids phytoplankton growth by supplying bottom-layer nutrients into the subsurface chlorophyll maximum but reduces phytoplankton concentrations in the thermocline by mixing cells from the base of the subsurface maximum into the bottom mixed layer. The turbulent dissipation observations were used to estimate an average nitrate flux into the thermocline of 2.0 (0.8–3.2, 95% confidence interval) mmol m⁻² d⁻¹, which is estimated to have been capable of supporting new phytoplankton growth at a rate of 160 (64–256) mg C m⁻² d⁻¹. Turbulent entrainment of carbon from the base of the subsurface biomass maximum into the bottom mixed layer was observed to be 290 (120–480) mg C m⁻² d⁻¹. This apparent excess export from the chlorophyll maximum is suggested to be a feature of the spring-neap cycle, with export dominating as the tidal turbulence increases toward spring tides and erodes the base of the thermocline. The observed rate of carbon export into the bottom mixed layer could account for as much as 25% of the gross annual primary production in stratifying shelf seas. Such turbulent losses, combined with grazing losses and low light levels, suggest that phytoplankton need to be highly adapted to environmental conditions within the thermocline in order to survive.

The seasonal thermocline is an important physical barrier in the ocean, separating the surface mixed layer from the deeper water. The stability of the vertical temperature (density) gradient inhibits diapycnal transfer of properties (e.g., momentum, heat, nutrients, algal cells, and oxygen). As the transition region between the nutrient-poor, well-lit surface layer and the darker, nutrient-rich deeper water, the thermocline plays a role in determining the biological properties of the water column. Since the development of continuous fluorescence measurements as a technique for observing the vertical structure of algae (Lorenzen 1966), the thermocline has been observed to be a region of enhanced chlorophyll concentration (e.g., Anderson 1969; Cullen and Eppley 1981; Holligan et al. 1984). Observed concentrations of subsurface chlorophyll range between 0.5 mg m⁻³ in the open ocean up to 100 mg m⁻³ in shelf seas. Although in some cases this higher chlorophyll concentration has been shown to be the result of a lower carbon:chlorophyll ratio (Steele

1964), most studies show this subsurface chlorophyll maximum to represent a real maximum in phytoplankton biomass.

The vertical position of the chlorophyll maximum is generally close to the maximum density gradient. It has been suggested that such accumulation of phytoplankton is the result of nutrient-dependent sinking of cells (Steele and Yentsch 1960). However, chlorophyll maxima have a higher correlation with the nitracline than with the thermocline (Cullen and Eppley 1981). Furthermore, both observations and modeling have shown that the flux of nitrate down the nitracline can support in situ growth of phytoplankton at the subsurface maximum (Jamart et al. 1977; Fairbanks and Wiebe 1980; Varela et al. 1992; Sharples and Tett 1994). This localized growth within the thermocline has been observed to account for 20%–30% of total water column primary production (Revelante and Gilmartin 1973). Considering that production in the subsurface maximum uses the diapycnal source of nitrate, whereas production further up in the water column relies on recycled nitrogen, it is likely to be an important region of new production (Goering et al. 1970; Probyn et al. 1995).

Given that a considerable proportion of the world's oceans has either a permanent or seasonal near-surface thermocline, an understanding of new production within and export from the various subsurface chlorophyll maxima is an important

¹ Corresponding author (j.sharples@soc.soton.ac.uk).

Acknowledgments

Ray Wilton (University of Wales, Bangor) provided invaluable technical support for FLY. Our thanks to the crew and RVS support staff on RRS *Challenger* during cruise CH145. This work was funded by the Natural Environment Research Council grant GR3/11829.

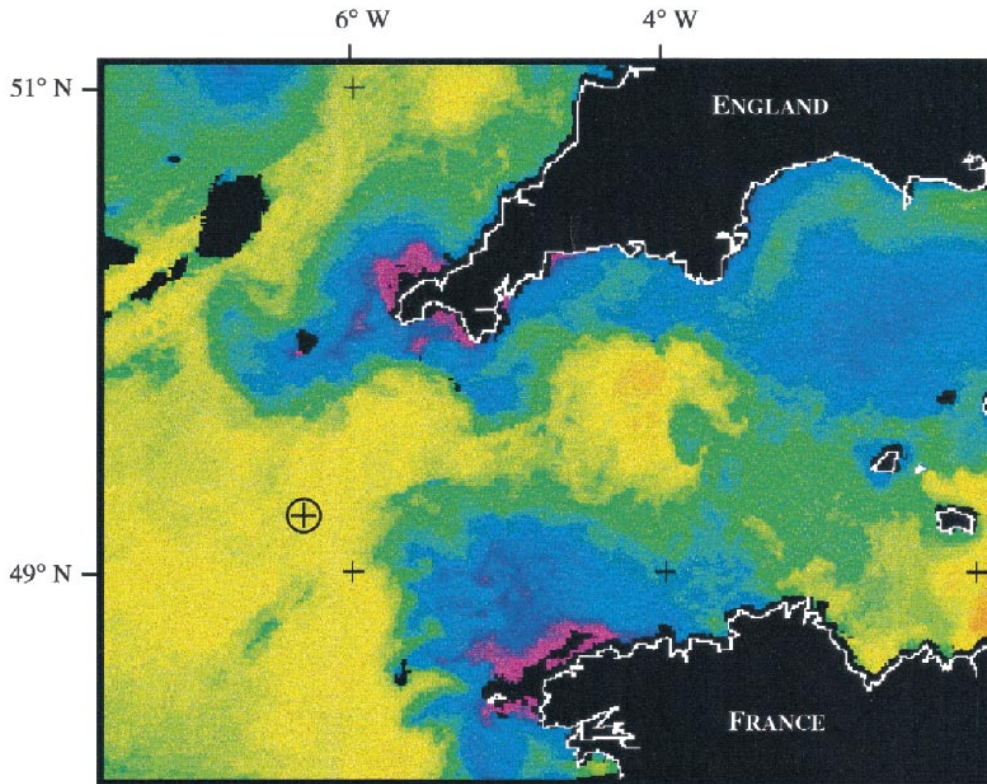


Fig. 1. AVHRR sea surface temperature image of the western English Channel (0344 h on 24 July 1999). Purple and blue colors (14–15°C) indicate well-mixed water, and green and yellow (17–18°C) indicate the temperature of the surface mixed layer of a stratified water column. ⊕ marks the position of the time series station. Advanced Very High Resolution Radiometer (AVHRR) data were received by the NERC Dundee Satellite Receiving Station and processed by the Remote Sensing Data Analysis Service (Plymouth Marine Laboratory).

requirement in our attempts to quantify carbon fluxes within the ocean (e.g., Sathyendranath et al. 1991). Here we present observations of turbulent dissipation rates and concentrations of chlorophyll that highlight the processes that both fuel and remove primary producers in a highly concentrated (5–80 mg chlorophyll $a\ m^{-3}$) shelf sea subsurface chlorophyll maximum. The observations of such high levels of subsurface biomass highlight the remarkable ability of phytoplankton to adapt to their surroundings. Combining the observations of phytoplankton biomass and turbulence dissipation shows how tidal turbulence in the bottom mixed layer both supplies new nitrogen into the base of the thermocline and periodically removes large amounts of phytoplankton from the subsurface maximum to respire in the bottom water and be consumed by herbivores. We suggest that this flux represents an important summer carbon flux out of the subsurface chlorophyll maximum, invisible to remote-sensing methods for estimating export productivity.

Methods

A single station was occupied by the RRS *Challenger* in the well-stratified western English Channel (Fig. 1) between 1345 h on 8 August and 1510 h on 9 August 1999. Neap tide had occurred 2 d earlier, on 6 August, and spring tides

were due on 13 August. All times are quoted as universal coordinated time (UTC) (equivalent to Greenwich mean time). Vertical profiles of salinity and temperature were made with a Neil Brown MKII conductivity, temperature, depth (CTD) probe, with a Chelsea Instruments MKII Aquatracka chlorophyll fluorometer providing information on the vertical chl a distribution. A Valeport SUV-6 in situ spectrophotometer (see Finch et al. 1998) was also interfaced with the CTD, to provide vertically well-resolved profiles of nitrate through the water column.

Water samples were collected for standard salinity calibration of the CTD, with subsequent analysis of the samples allowing calibration of the CTD salinity to ± 0.003 (PSS78). Continuous checks of the CTD temperature were made against two calibrated SIS reversing thermometers, with the CTD temperature then being calibrated relative to the reversing thermometers to $\pm 0.002^\circ\text{C}$. Chl a concentrations were measured by filtering sampled water through Whatman GF/F filters and analyzed following the method of Welschmeyer (1994). Every time water was collected for chl a analysis, a sample was also fixed with Lugol's iodine for later phytoplankton species identification. Water samples were also analyzed for nitrate concentration. Nitrate samples were determined on board by use of a Burkard AA-II type autoanalyzer, employing the standard sulphanilimide and nap-

thyl-ethylene diamine dihydrochloride method (Grasshoff et al. 1983).

The Aquatracka chlorophyll fluorometer was calibrated by comparing the fluorometer output voltage with the chl *a* concentrations measured in the corresponding water samples. The discrete chlorophyll samples covered a range of concentrations between the very low surface water values of 0.3 mg m⁻³ and high thermocline values of up to 40 mg m⁻³. The amplifier within the Aquatracka is designed so that the voltage output changes by 1 V per decade increase in chlorophyll, making it particularly suitable to the wide range of chlorophyll concentrations observed in this study. A regression of the log-transformed chl *a* concentrations against the fluorometer output (in V) yielded a calibration equation of

$$\text{Calibrated chlorophyll } a = 0.04e^{2.70V} \quad [\text{mg chl m}^{-3}], \quad (1)$$

($N = 40$, $r^2 = 0.89$, $P < 0.001$). The root-mean square percentage scatter of the chl *a* samples about this regression is $\sim 30\%$. One frequent source of scatter in in situ fluorometer calibrations is the day-night variability of chlorophyll fluorescence associated with quenching of the fluorescence response in well-lit surface waters (e.g., Strass 1990). This is unlikely to be a factor in the present work, since most of the chlorophyll was situated within the thermocline, at a depth of ~ 30 meters. Instead, the uncertainty is the result of attempting to sample thin layers of concentrated chlorophyll (often only 1–3 m thick) with a standard CTD and bottle rosette system. Because the rosette bottles were themselves 1 m long and situated ~ 1 m above the fluorometer, it can be difficult to associate reliable fluorometer voltages with these localized and patchy chlorophyll layers. Vertical profiles of chl *a* have all been calculated by applying equation (1) to the CTD fluorometer data.

Observations of turbulent kinetic energy dissipation were made using the FLY (Free-fall Light Yoyo) shear profiler (Dewey et al. 1987). FLY falls through the water column at a speed of ~ 80 cm s⁻¹, providing measurements of velocity shear on a scale of ~ 1 cm. Dissipation estimates were made using

$$\varepsilon = 7.5\nu \overline{\left(\frac{\partial u}{\partial z}\right)^2} \quad [\text{m}^2 \text{s}^{-3}], \quad (2)$$

with ν the kinematic viscosity of seawater. The mean square shear was calculated following Simpson et al. (1996), who estimate the instrumental error in calculating ε to be 50%. One set of FLY dissipation data consisted of five consecutive profiles, taking a total of ~ 20 minutes. The profiles were then averaged and turbulent dissipation calculated every 5 m through the water column. The variability in the dissipation estimates is demonstrated by calculating the 95% confidence using a bootstrapping technique (Efron and Gong 1983). The profile of vertical eddy diffusivity, K_z , was then derived using the dissipation method of Osborn (1980) via

$$K_z = \frac{R_f}{1 - R_f} \frac{\varepsilon}{N^2} \quad [\text{m}^2 \text{s}^{-1}], \quad (3)$$

with N the Brunt-Vaisala frequency, and the factor $R_f/(1 - R_f)$ is taken to be equal to 0.2 (e.g., Osborn 1980; Mounm 1996).

One complete set of observations consisted of the series of five consecutive profiles with FLY, followed by one CTD cast. On average, including repositioning of the ship between sets of observations, such a FLY-CTD pair, took 70 min to complete.

A vessel-mounted RDI narrowband 150 kHz Acoustic Doppler Current Profiler (ADCP) was operated continuously throughout the station, providing vertical profiles of current velocity between depths of 11 and 103 m with a 4-m bin size. Raw data was collected in 4-ping ensembles, with each ensemble taking just over 4 s to collect. The raw data were then processed to provide 5-min average velocity profiles. Standard deviation of this averaged data was < 1 cm s⁻¹.

Results

A typical profile of the data, taken at 1215 h on 9 August 1999, shows the position of the chlorophyll maximum in relation to the sharp two-layered physical structure of the water column (Fig. 2). Surface and bottom water salinities were 35.2 and 35.3, respectively, so that density was controlled primarily by the thermal structure of the water column. The profile of temperature (Fig. 2a) shows the typical two-layer structure often found in stratified, tidally energetic shelf seas. The strength of the tidal turbulence in the bottom mixed layer is illustrated by the very low temperature variance recorded; the mean temperature in the water deeper than 40 m was $11.164 \pm 0.002^\circ\text{C}$. A very sharp thermocline separated these two mixed layers, with a maximum temperature gradient of 2°C m^{-1} . A typical value for the temperature gradient over the whole time series was $\sim 1^\circ\text{C m}^{-1}$.

A narrow subsurface chlorophyll maximum was situated in the lower half of the thermocline (Fig. 2b), with a vertical thickness of ~ 5 meters. This thermocline concentration of chl *a* was highly variable during the time series. Peak values within the subsurface maximum reached as high as 80 mg m⁻³. The average maximum concentration over the entire time series was 26 mg m⁻³, though the median was 13 mg m⁻³ reflecting the contribution of a small number of high concentration patches in the mean. This biomass maximum was, both within and outside concentrated patches, dominated by a small (10–15 μm) coccolithophore, *Calyptrosphaera oblonga* (D. Harbour, pers. comm.). In the surface mixed-layer chl *a* concentrations were low (0.1–0.3 mg m⁻³), whereas in the bottom mixed layer there was a depth-uniform concentration of ~ 0.5 –1 mg m⁻³. Low surface layer chlorophyll, a high subsurface chlorophyll maximum, and low but significant bottom-layer chlorophyll was a consistent feature illustrated by all of the chlorophyll profiles and discrete samples taken during the 25-h station. Data from a downwelling photosynthetically available radiation (PAR) sensor on the CTD was used to calculate an average vertical attenuation coefficient for PAR over the time series of $k = 0.09 \text{ m}^{-1}$, so that the 1% PAR depth was at 50 meters (i.e., well below the thermocline and the subsurface biomass maximum). The biomass maximum was thus located at the 5% light level.

The nitrate sample data demonstrated the classic pattern of a well-stratified, temperate shelf sea in summer, with un-

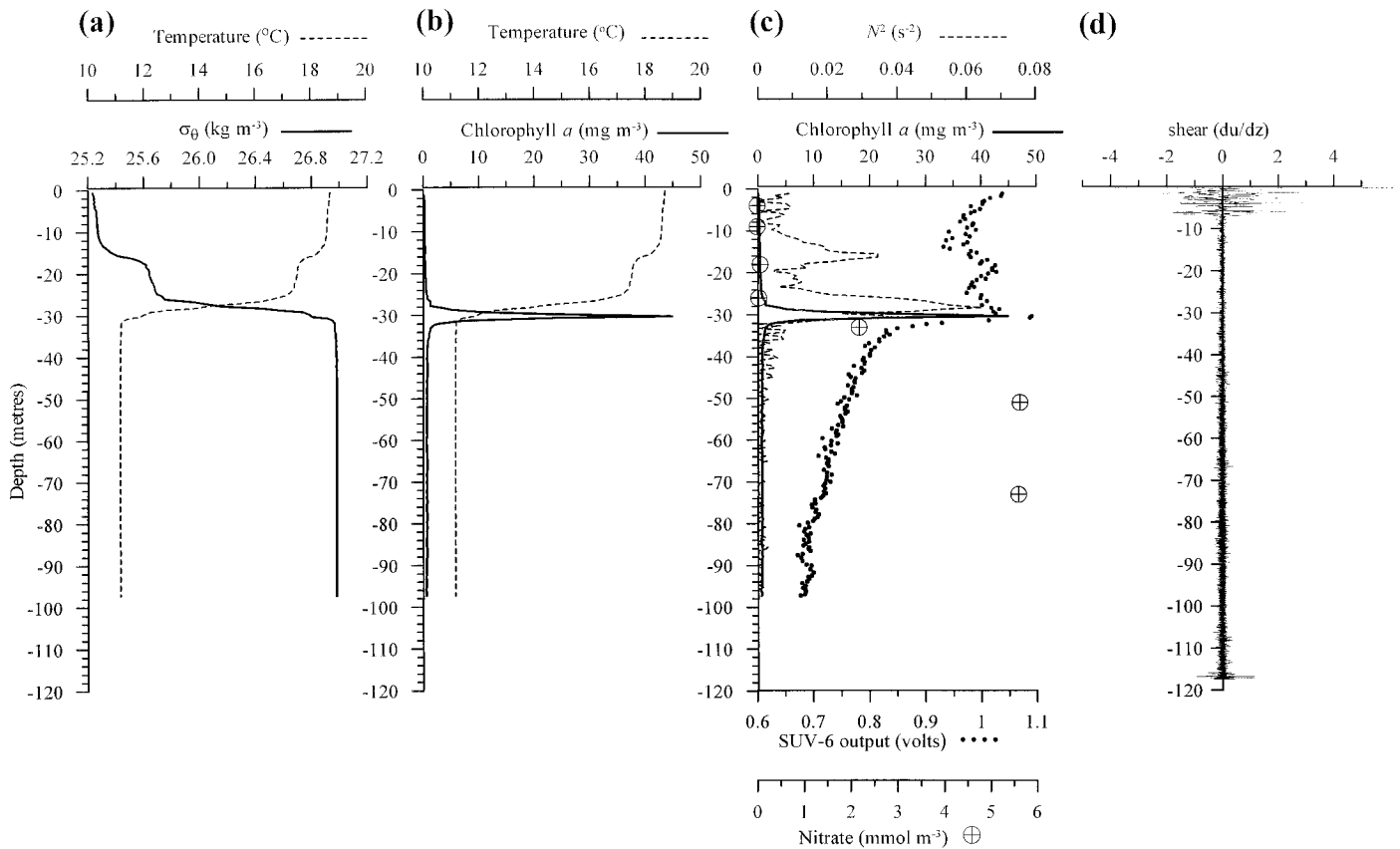


Fig. 2. Water column structure at 1215 h on 09 August 1999. (a) Temperature (°C) and σ_θ (kg m⁻³). (b) Temperature (°C) and chlorophyll *a* concentration (mg m⁻³). (c) Chl *a* concentration (mg m⁻³), squared Brunt-Vaisala frequency (s⁻²), nitrate concentrations from water sample analysis (mmol m⁻³), and the raw output from the SUV-6 in situ spectrophotometer. (d) An example of raw current shear data from FLY. The upper 10 meters are normally ignored, as the signal is entirely caused by the ship's wake. The data were collected at 1145 h on 09 August 1999, as tidal flow was increasing and show the higher variability associated with bed stress.

detectable nitrate levels in the surface layer and high nitrate (almost 6 mmol m⁻³) in the bottom mixed layer (Fig. 2c). However, although the voltage output from the SUV-6 spectrophotometer, which is inversely related to nitrate concentration, showed the correct qualitative behavior (Fig. 2c), drift in the sensor output prevented any realistic attempts at calibration. A key requirement of this work was to measure the vertical flux of nitrate via

$$\text{nitrate flux} = -K_z \left(\frac{\Delta N}{\Delta z} \right) \quad [\text{mmol N m}^{-2} \text{ s}^{-1}], \quad (5)$$

where ΔN is the difference between surface and bottom layer nitrate concentration, Δz is the thickness of the nitracline, and K_z is the vertical eddy viscosity provided by the FLY results. Given that surface nitrate was undetectable throughout the time series, and bottom layer nitrate was approximately constant at 5.7 mmol m⁻³, ΔN can be taken to be constant at 5.7 mmol m⁻³. Despite the inability to calibrate the SUV-6, the down-cast data from the sensor did show that the upper edge of the nitracline was consistently coincident with the peak of the subsurface chlorophyll maximum (e.g., Fig. 2c). However, the SUV-6 sampling protocol meant that it was not possible to identify the base of the nitracline from the output. Data were output by the instrument at 1Hz, but

each data point was a running average over the previous 8 s. Thus, during the down-cast, the output from the sensor would represent a smoothed version of the nitracline, beginning coincident with the upper part of the nitracline but extending beyond the base of the nitracline. At a CTD lowering rate of 0.5 m s⁻¹, the true bottom layer nitrate would not be reached by the SUV-6 until 4 m below the base of the nitracline, which would result in a significant underestimate of the nitrate gradient. In principle, the data during the up-cast would have the opposite problem and therefore provide an indication of where the base of the nitracline started. However, within such sharp vertical gradients, the up-cast data were unreliable because of the mixing caused by the passage of the CTD and bottle rosette through the water ahead of the CTD sensors. The depth of the base of the nitracline was estimated by considering that the intensity of the turbulence in the bottom mixed layer would be unlikely to result in the existence of a significant nitrate gradient without a concomitant observation of a temperature gradient. The thickness of the nitrate gradient was therefore taken to be between the peak of the subsurface chlorophyll and the top of the bottom mixed layer. This corresponds with the results of Holligan et al. (1984), who estimated the extent of the nitracline in the western English Channel by use of continuous obser-

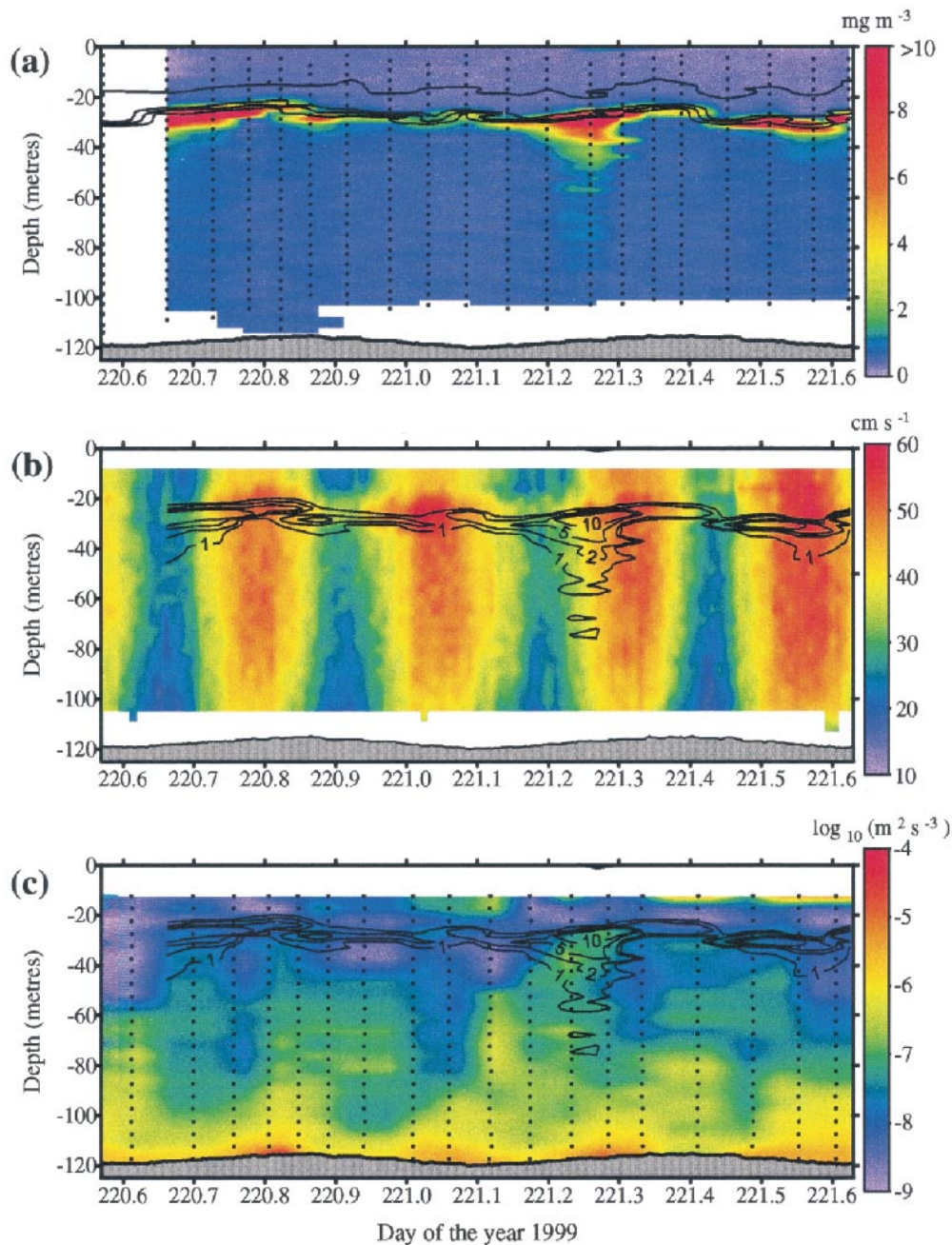


Fig. 3. Time series of vertical water column structure between 1345 h on 08 August and 1510 h on 09 August 1999. (a) Temperature ($^{\circ}\text{C}$, lines) contoured every 2°C and chlorophyll *a* concentration (mg m^{-3} , colored). The vertical dotted lines mark the times of the CTD casts. (b) Chl *a* concentration (lines) contoured at 1, 2, 5, and 10 mg m^{-3} , and current speed (cm s^{-1} , colored) from the vessel-mounted ADCP. (c) Chl *a* concentration (lines) contoured at 1, 2, 5, and 10 mg m^{-3} , and turbulent energy dissipation ($\log_{10}(\text{m}^2 \text{s}^{-3})$, colored) from the FLY profiler. The vertical dotted lines mark the mean times of each of the groups of FLY casts.

variations of nitrate, temperature, and chlorophyll from a pumped supply from an intake on their CTD. In the observations presented here this results in Δz varying typically only between 1 and 3 m during the time series, and thus the nitrate gradient was between 5.7 and 1.9 mmol m^{-4} .

A profile of the raw shear data from a FLY profile (Fig. 2d) illustrates the dominance of nearbed shear. It also high-

lights the problem of near-surface contamination by the ship's wake. To avoid this, all analysis of the FLY data subsequently ignored the upper 10 m of the water column.

The thermocline remained at a constant depth of approximately 30 m (Fig. 3a). The subsurface chlorophyll maximum was always situated within the base of the thermocline (Fig. 3a), the peak of the subsurface chlorophyll maximum

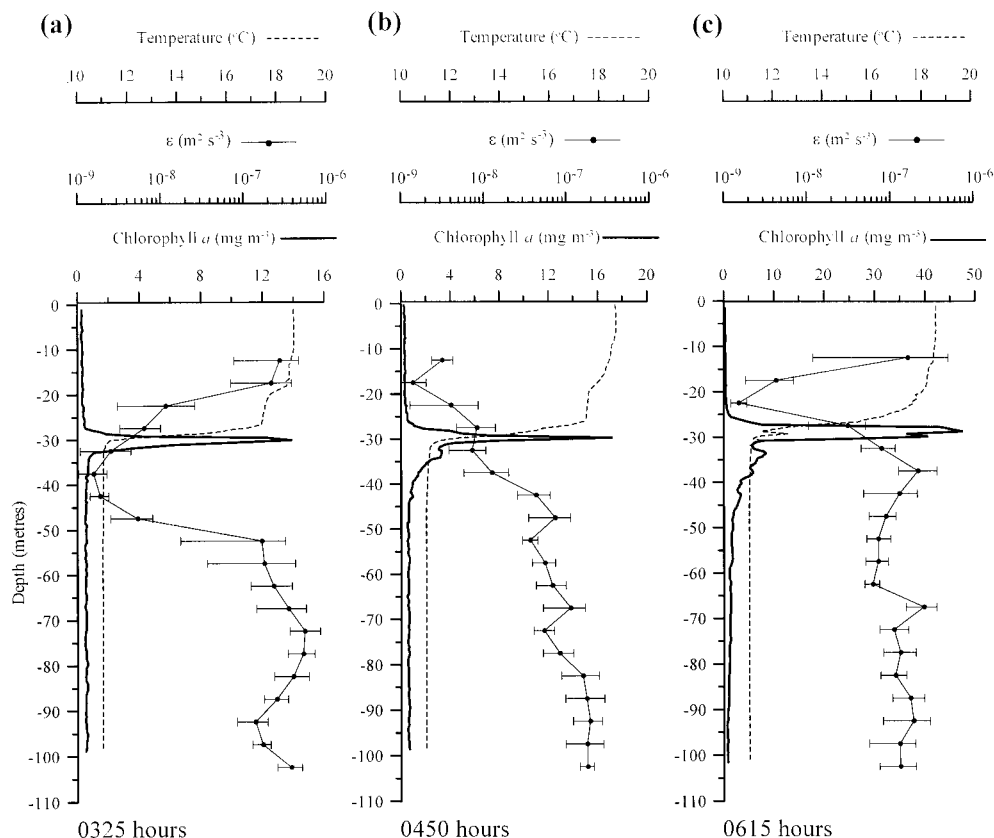


Fig. 4. Vertical distributions of chlorophyll a (mg m^{-3}), turbulent energy dissipation ($\text{m}^2 \text{s}^{-3}$), and temperature ($^{\circ}\text{C}$) prior to and during the mixing event at 0600 h on 09 August. Error bars on the dissipation profiles mark the 95% confidence limits. (a) CTD data from 0325 h, FLY data from 0250 h. (b) CTD data from 0450 h, FLY data from 0410 h. (c) CTD data from 0615 h, FLY data from 0535 h.

being situated consistently ~ 1 m below the stability maximum throughout the time series. There were at least two occasions when significant concentrations of chlorophyll were observed reaching from the base of the thermocline into the bottom mixed layer (at times 220.67 and 221.26 d in Fig. 3a). Tidal currents reached a maximum of 60 cm s^{-1} (Fig. 3b). Maximum observed turbulent dissipation rates (Fig. 3c) reached $\sim 3 \times 10^{-5} \text{ m}^2 \text{ s}^{-3}$ near the seabed, at the same time as maximum nearbed tidal currents (Fig. 3b). Maximum dissipation occurred later higher up in the water column, with maximum dissipation at the thermocline (~ 90 m above the seabed) occurring ~ 5 h after the peak in nearbed dissipation. This phase lag of dissipation away from the bottom boundary is thought to be driven by the vertical progression of the region of maximum shear during the tidal cycle (Simpson et al. 2000). Minimum values of turbulence dissipation rates were always found within the thermocline, typically between 10^{-8} and $10^{-9} \text{ m}^2 \text{ s}^{-3}$ (the noise level of the FLY measurements is equivalent to a dissipation of $\sim 3 \times 10^{-10} \text{ m}^2 \text{ s}^{-3}$).

The two occasions when higher concentrations of chlorophyll were seen to reach into the bottom mixed layer appear correlated with times when there was an increase in the turbulent dissipation at the base of the thermocline. This is particularly obvious at time 221.26 d, when the turbulent

dissipation rate increased to $\sim 3 \times 10^{-7} \text{ m}^2 \text{ s}^{-3}$ at the same time that a large amount of chlorophyll was observed below the thermocline. The implication is that this observation recorded in Fig. 3c represents turbulent entrainment of phytoplankton from the base of the subsurface biomass maximum down into the deeper water. This is further illustrated by considering the profiles of temperature, chl a , and turbulence dissipation leading up to the entrainment event (Fig. 4a–c). Between the two sets of data in Fig. 4a and c, turbulent dissipation at the base of the thermocline increased by almost two orders of magnitude. Using equation (3), the estimated vertical diffusivity in the base of the thermocline (i.e., at a depth of 32 m) increased from $4 \times 10^{-6} \text{ m}^2 \text{ s}^{-1}$ to $5 \times 10^{-5} \text{ m}^2 \text{ s}^{-1}$. If we ignore the correspondence between the appearance of chlorophyll in the bottom mixed layer and the increased dissipation at the base of the thermocline, an alternative explanation for this is the advection of a locally high concentration of biomass within the deep water. However, although advection certainly played a role in varying the total water column chlorophyll beneath the ship, the vertical distribution of chlorophyll in the bottom mixed layer requires an alternative explanation. The chlorophyll observations during the main mixing event (Fig. 3) show a marked decrease in chlorophyll concentration away from the base of the thermocline. An estimate of the mixing time scale, t ,

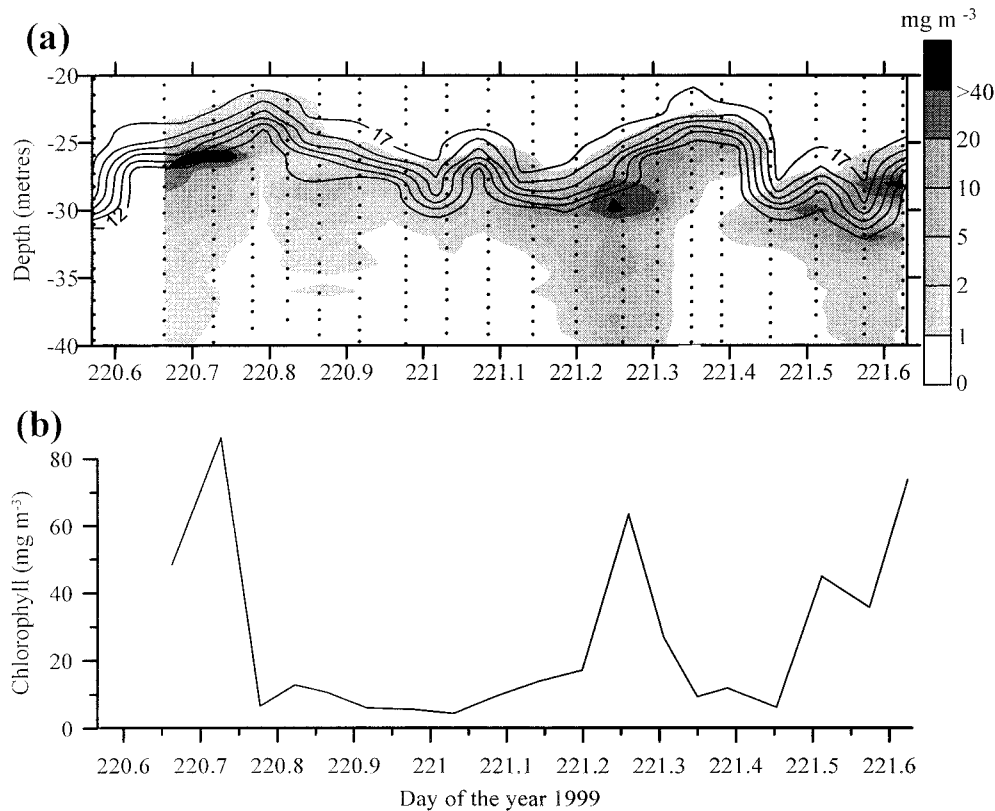


Fig. 5. (a) Detailed view of the time series of temperature ($^{\circ}\text{C}$, lines) and chlorophyll *a* concentration (mg m^{-3} , shaded) at the thermocline. (b) Time series of the maximum chl *a* concentration (mg m^{-3}) within the thermocline.

within this tidally mixed bottom layer can be made using $t \approx L^{2/3} \varepsilon^{-1/3}$ (Denman and Gargett 1983), with L a mixing-length scale taken to be half the thickness of the bottom mixed layer (35 m). Using a typical value of ε in the bottom layer of $2 \times 10^{-7} \text{ m}^2 \text{ s}^{-3}$ gives a mixing time of 30 min. Thus, within this energetic mixed layer, such vertical heterogeneity will be short-lived, and again the implication is that the biomass distribution is the result of active, or very recent, mixing out of the subsurface chlorophyll maximum.

The detailed distribution of chlorophyll within the subsurface maximum is illustrated by expanding the thermocline region (Fig. 5). The two main entrainment events (times 220.67 and 221.26 d) are clear, with two other events (times 220.87 and 221.5 d) also apparent. These latter two events can be seen in Fig 3c, penetrating less deeply into the bottom mixed layer but both associated with increases in the turbulent dissipation rate at the base of the thermocline. The variability of the peak chlorophyll concentration within the subsurface maximum (Fig. 5b) shows two main peaks separated by ~ 12 h, suggesting tidal advection of a particularly concentrated patch past the position maintained by the ship. Between these peaks, chl *a* concentrations ranged from 5 to 20 mg m^{-3} , with the return of high concentrations at the end of the time series. If we assume that patches had a typical lifetime of 2–3 h in the time series, and average current speeds were $\sim 30 \text{ cm s}^{-1}$, then the length scale of the patches can be estimated to be of the order of 2–3 km. Assessing

the horizontal scale of this patchiness is, however, difficult with such a short set of observations made at one point in space, so a more cautious estimate would be 1–10 km.

Discussion and conclusions

Growth of phytoplankton requires sufficient supplies of light and nutrients. Growth within the subsurface maximum therefore requires the thermocline to be situated above the compensation depth and a flux of nutrients into the base of the thermocline. Our observations show a concentrated, patchy, monospecific layer of phytoplankton within the thermocline, situated above the 1% light level. Mean irradiance at a depth of 30 m during the observations was 4 W m^{-2} ($\sim 18 \mu\text{E m}^{-2} \text{ s}^{-1}$) averaged over 24 h, or 6 W m^{-2} ($27 \mu\text{E m}^{-2} \text{ s}^{-1}$) over the daylight period. Although data are not available on the compensation light requirements of *C. oblonga*, Brand and Guillard (1981), have recorded other species of coccolithophores achieving growth rates of ~ 1 doubling per day at an irradiance of 7 W m^{-2} . It would appear, therefore, that there was sufficient irradiance at the thermocline for photosynthesis to take place.

By combining our measurements of the strength of the nitrate gradient and of the vertical eddy diffusivity at the position of the maximum nitrate gradient, we can calculate the flux of nitrate into the base of the thermocline using equation (4). In this case, K_z was recalculated with a vertical

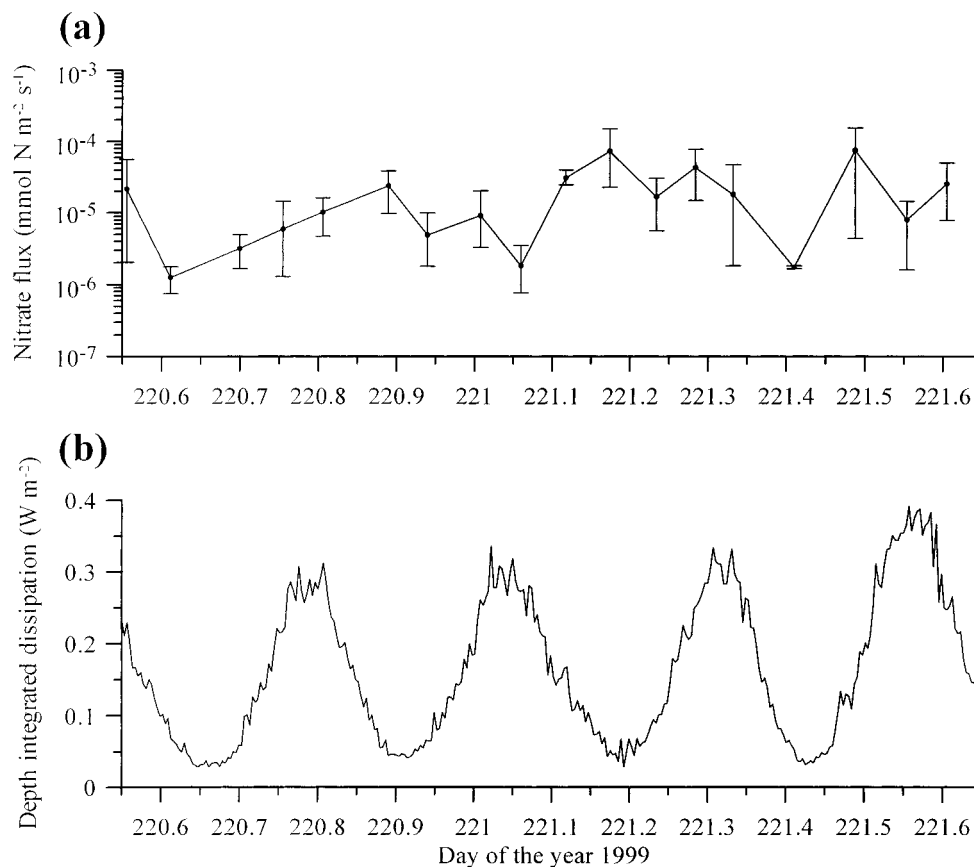


Fig. 6. (a) Time series of the vertical nitrate flux through the nitracline ($\text{mmol nitrate m}^{-2} \text{s}^{-1}$). Error bars mark the 95% confidence limits. (b) Estimated depth-integrated tidal energy dissipation (W m^{-2}), $k_b \rho \bar{u}^3$, with $k_b = 0.0025$, ρ (kg m^{-3}) the bottom water density, and \bar{u} (m s^{-1}) the depth-averaged current speed from the ship's ADCP.

resolution of 2 m (i.e., on the same scale as the vertical extent of the nitracline) and forcing a 2-m bin to be centered on the nitracline of each CTD cast. A value of the flux was calculated for each individual CTD cast by use of the nitrate gradient provided by that CTD cast and a value for K_z from the associated ensemble of five FLY casts. The resulting time series of vertical nitrate flux (Fig. 6a) suggests some variability associated with the tidal energy dissipation (Fig. 6b), although the uncertainties in the flux measurements preclude any definitive conclusions.

Integrating the nitrate flux over the entire time series in Fig. 6a yields an average supply of nitrate into the base of the thermocline of ~ 2.0 ($0.8\text{--}3.2$, 95% confidence interval) $\text{mmol m}^{-2} \text{d}^{-1}$. In the western English Channel, this can be compared with an estimate of diapycnal nutrient flux made on the basis of several years of temperature and phosphate data by Pingree and Pennycuik (1975). They estimated summer vertical diffusivities at the thermocline to be $\sim 1 \times 10^{-4} \text{ m}^2 \text{ s}^{-1}$. Converting their mean summer vertical phosphate gradient into a nitrate gradient, under the assumption of the Redfield N:P ratio, suggests a mean summer vertical flux of $1.5 \text{ mmol N m}^{-2} \text{ d}^{-1}$, consistent with our results from the dissipation-based flux calculation. An observational estimate, using similar methods to those we have presented here, has been carried out in stratified shelf water on Georges

Bank (Horne et al. 1996). There the mean cross-thermocline nitrate flux was found to be typically $3\text{--}11 \text{ mmol m}^{-2} \text{ d}^{-1}$. Both the Horne et al. estimate of nitrate flux and our estimate presented in this work have large errors associated with them, primarily resulting from the uncertainties involved in the dissipation measurements. The relatively low value suggested for the western English Channel, compared with Georges Bank, is likely to be due to the strong stratification. It is also worth comparing this nitrate supply rate that fuels shelf sea thermocline phytoplankton populations to the rates of supply to subsurface populations in the far less energetic environment of the open ocean. Lewis et al. (1986) measured a vertical nitrate flux into the nitrate-poor surface oligotrophic ocean of $\sim 0.14 \text{ mmol m}^{-2} \text{ d}^{-1}$. Planas et al. (1999) have recently estimated vertical nitrate fluxes of $\sim 0.5 \text{ mmol m}^{-2} \text{ d}^{-1}$ associated with equatorial upwelling and as low as $\sim 0.05 \text{ mmol m}^{-2} \text{ d}^{-1}$ in the North Atlantic subtropical gyre. Vertical turbulent fluxes of nitrate into shelf sea thermoclines appear to be at least an order of magnitude higher than those found in the open ocean, providing the mechanism for the higher production rates and biomass concentrations seen in shelf sea subsurface biomass maxima.

The decoupling of the thermocline and nitracline (e.g., Holligan et al. 1984) can be understood in terms of uptake by the phytoplankton removing much of the nitrate from

regions of high cell concentrations and thus both deepening and sharpening the nitrate gradient. This biological control on the nitrate gradient has the advantage for the phytoplankton of increasing the nitrate flux. If, for instance, the phytoplankton actively attempted to maintain a position more closely associated with the region of maximum stability (i.e., 1 m above the observed position), then the nitrate gradient would be reduced by a factor of 1.5–2, similarly reducing the nitrate flux. However, although the passive link between the biomass maximum and the nitracline will enhance nitrate flux, it also results in a gradual deepening of the nitracline and biomass maximum within the thermocline. This increases the danger of cells being mixed out of the base of the subsurface chlorophyll maximum at times of increased turbulent dissipation and thus being removed permanently from the photic zone. The time series of turbulent dissipation and chlorophyll (Fig. 3c) showed one particularly dramatic example that demonstrates this tenuous existence led by the phytoplankton. Using the chlorophyll data in Fig. 4c and assuming that the bottom mixed layer had a uniform concentration of $1 \text{ mg chl } a \text{ m}^{-3}$ prior to the mixing event, it can be estimated that the additional chlorophyll found in the bottom mixed layer constituted $\sim 35\%$ of the total chlorophyll that would have been in the subsurface maximum before the event. Integrating this additional bottom mixed layer chlorophyll indicates that this single mixing event removed $\sim 80 \text{ mg chl m}^{-2}$. Direct measurement of the C:chl ratio of these cells was not possible. Fernández et al. 1996, have reported C:chl ratios between 30 and 60 for the coccolithophorid *Emiliana huxleyi* when grown under light-limited conditions. Under the assumption that the high concentrations of *C. oblonga* suggest the cells to be well-adapted to the low light levels at the thermocline, we use a C:chl ratio of 30, which implies a carbon flux into the bottom layer of 2.4 g C m^{-2} . However, considering that the observed concentration of chl *a* within the subsurface maximum varied considerably during the time series, it is likely that this large carbon flux was simply a consequence of the ship being positioned over a patch of high chlorophyll concentration at the time of the turbulence increase at the base of the thermocline. We can estimate a time series of the carbon flux in the same way as the nitrate flux was calculated, using the chlorophyll gradient provided by each CTD cast. The daily mean flux can again be calculated by taking the mean of the time series of individual fluxes. Under the assumption of the C:chl ratio of 30, the mean carbon flux implied by the observations is calculated to be ~ 290 (120–480, 95% confidence interval) $\text{mg C m}^{-2} \text{ d}^{-1}$. Note that here it has been assumed that *C. oblonga* is neutrally buoyant within the subsurface maximum. Over the time series, this can be justified by considering the variability of the position of the chlorophyll maximum about the mean density at which it was observed, $\sigma_\theta = 26.8 \pm 0.1 \text{ kg m}^{-3}$, corresponding to a vertical variation within the thermocline of less than $\pm 0.5 \text{ m}$. Alternatively, we can consider the potential flux of cells out of the subsurface maximum assuming a sinking rate of 1 m d^{-1} . Taking a mean thickness of the subsurface maximum of 5 m and a typical concentration of chlorophyll of 10 mg m^{-3} , suggests a daily flux of $120 \text{ mg C m}^{-2} \text{ d}^{-1}$, potentially half of the turbulent export. However, without any detailed

knowledge of the possible buoyancy control or motility of *C. oblonga*, we will continue with the assumption of neutral buoyancy.

Both the calculations of nitrate and carbon flux are an attempt to quantify a daily averaged diffusive flux as $-K_z(\partial C, N/\partial z)$, where the values for the diffusivity and the concentration gradients form a time series of instantaneous measurements. Entrainment of thermocline water into the bottom mixed layer, and of nutrient-rich bottom water into the thermocline, is clearly an event-scale process (i.e., consider the patchy mixing of chlorophyll into the bottom mixed layer, Fig. 3). The results in Fig. 6, however, suggest that the combination of hourly FLY and CTD profiling is not sufficient for quantifying this temporal variability. Combining free-fall turbulence measurements and gradients calculated from separate CTD profiles could result in underestimates of fluxes because of a mismatch between a dissipation measurement and a vertical gradient after it has been acted on by that turbulence. The solution to this problem is simply to measure both diffusivity and scalars with instruments on the same free-falling package. Collecting data from a drifting ship potentially introduces spatial variability to the estimates of uncertainty, which may complicate our attempt at calculating a mean local flux. However, the region of the western English Channel where the present data was collected has uniform bathymetry and a horizontally uniform (on scales greater than a tidal excursion) tidal current and temperature structure, so it is reasonable to assume some spatial homogeneity in the turbulence. The uncertainty is expected to be dominated, in this case, by the time variability of turbulent events. Finally, and more speculatively, it is perhaps worth considering the temporal resolution of the FLY data. Recent observations of turbulence in shallow coastal waters (Nimmo Smith et al. 1999) suggest that this could be similar to the timescale of the variability of turbulent events driven by tidal stress at the seabed. Thus, it is possible that the FLY casts could miss extremes of turbulence and lead to underestimates of turbulent fluxes.

Under the assumption that the uncertainties discussed above will affect our estimates of carbon and nitrate fluxes in a similar fashion, we now attempt to ascertain whether or not the new production fuelled by the tidally driven diapycnal nitrate flux is sufficient to compensate for the losses of phytoplankton into the bottom mixed layer. The nitrate observations showed that none of the measured flux entered the surface water, so we can speculate that this flux represents the potential new nitrate uptake rate of the phytoplankton in the subsurface chlorophyll maximum. In the same region of the western English Channel, Le Corre and L'Helguen (1993) observed a nitrate uptake rate in the thermocline of $0.02 \text{ mmol m}^{-3} \text{ hr}^{-1}$. Under the assumption of a thickness of the subsurface chlorophyll maximum of 5 m , this would be equivalent to $\sim 2.5 \text{ mmol m}^{-2} \text{ d}^{-1}$, consistent with our calculated supply rate. Taking a typical C:N ratio for phytoplankton of 6.6, we can therefore estimate that the rate of new production within the thermocline could be 160 (64–256, 95% confidence interval) $\text{mg C m}^{-2} \text{ d}^{-1}$. Under the assumption that this production is spread over a region of thickness 5 m , this suggests a production rate of $\sim 30 \pm 16 \text{ mg C m}^{-3} \text{ d}^{-1}$, which compares with estimates of between

10 and 20 mg C m⁻³ d⁻¹ for phytoplankton in the summer thermocline of the western English Channel made by Joint et al. (1986) and Joint and Pomroy (1988). Although the new production and carbon flux estimates have large errors associated with them, it would appear that the supply rate of nutrients may not be sufficient to maintain the phytoplankton population against the removal rate of 290 mg C m⁻² d⁻¹. This problem is made worse if we consider that the low light levels within the thermocline will result in low growth rates and that the development of high concentrations of chlorophyll brings with it the disadvantage of shading. Also, such concentrated regions of biomass are likely to be attractive to grazers. However, two tidal cycles of observations during the transition between neap and spring tides will not be indicative of the full physical dynamics affecting production and fluxes at the thermocline. As tidal currents increase from neap to spring tides, the rate of turbulent dissipation at the base of the thermocline will increase, thus eroding the stratification and leading to the fluxes we have described. Alternatively, between spring and neap tides we might expect these fluxes to be reduced, since the weakening tidal turbulence allows stratification to develop deeper in the water column. In principle, assuming that the carbon and nitrate concentration differences between the thermocline and bottom mixed layer stay approximately constant, the production-export imbalance will still exist. However, this redevelopment of stratification represents an additional source of new nitrate, since the deepening thermocline traps the high nitrate water at the top of the bottom mixed layer. If we assume that, on average, the thermocline reaches ~1 m deeper in the 7 d between spring and neap tides, then this suggests an effective nitrate flux of almost 1 mmol m⁻² d⁻¹, i.e., an additional 50% above that associated with the tidal mixing events. It is therefore possible that spring-neap modulation of tidal mixing also plays a significant role in maintaining primary production within the subsurface maximum.

The observations of the subsurface chlorophyll concentration showed a patchy distribution, with an estimate of the lengthscale of these patches being between 1 and 10 km. An interesting, and with the present data set unanswerable, question concerns the mechanism(s) behind this patchiness. In particular, what processes are responsible for producing localized patches of chlorophyll of 40–80 mg m⁻³ within a larger region where 5–10 mg m⁻³ is more usual? If we assume that, within the low light regime of the thermocline, the growth rate of the phytoplankton is about one doubling every 2 d, then such a patch would take around 6 d to develop from the “normal” background concentration. The most obvious physical process operating on a similar timescale is the modulation of turbulent fluxes and stratification driven by the spring-neap cycle. We would normally assume that the physical processes provide approximately the same potential for production over a large area, so it is not clear how spring-neap modulation of turbulence could lead to such small-scale horizontal patchiness, and we might instead look for a biological mechanism to generate the horizontal variability. The preserved samples of phytoplankton showed the subsurface maximum to be virtually monospecific, both within and outside the patches, so interspecies physiological

differences are unlikely. Horizontal variability in grazing pressure could be a candidate mechanism.

In summary, by combining results from a turbulence shear probe, a CTD with chlorophyll fluorometer, and observations of nitrate, we have shown how tidal mixing both generates new production by periodically supplying new nitrate and depletes phytoplankton numbers by entraining them into the bottom mixed layer. We have estimated the net flux of material out of the subsurface maximum to illustrate the potential importance of tidal entrainment of carbon from the subsurface chlorophyll maximum. Once phytoplankton are mixed into the deeper water they are lost from the production regions of the water column, and this process constitutes a one-way flux of carbon out of the photic zone. Such constant tidal pumping provides a mechanism for new production and carbon export flux throughout the summer. This has important implications for attempts to quantify production rates in shelf seas, particularly when we consider that one of our best methods for estimating shelf sea productivity and carbon flux is centred on remote sensing of the color of the sea surface. The periodic supply of new nitrate into the thermocline will result in variability in the production rates within the subsurface maximum. Standard incubation techniques used to measure primary production are unlikely to take such variability into account, and so simple extrapolation of the results of such experiments could lead to an underestimation of production. Similarly, the variability in the turbulent entrainment out of the base of the thermocline could represent a significant missing component of carbon export measurements. If we take a typical estimate of gross primary production in a stratifying shelf sea region of 100 g C m⁻² year⁻¹ (Tett et al. 1993), then over the summer months our estimate of turbulent carbon flux could represent a removal of between 10% and 40% of the total annual production.

The above results are applicable to tidally energetic shelf seas. More generally, the subsurface biomass maximum is a ubiquitous feature of much of the world's shelf and open seas. The existence of this production, at or near regions of physical stability, illustrates the importance of physical discontinuities in marine productivity (e.g., the ergoline hypothesis of Legendre et al. 1986). Interesting questions arise when we consider that populations of phytoplankton at the thermocline (in the case of the western English Channel, remarkably dense populations) are maintained despite very low light levels and, presumably, potentially high grazing pressures. These phytoplankton thus appear to be physiologically very well-tuned to their environment, and our continuing lack of any clear explanation for the nature of this adaptation represents a significant gap in our understanding of marine primary producers.

References

- ANDERSON, G. C. 1969. Subsurface chlorophyll maximum in the northeast Pacific Ocean. *Limnol. Oceanogr.* **14**: 386–391.
- BRAND, L. E., AND R. R. L. GUILLARD. 1981. The effects of continuous light and light intensity on the reproduction rates of 22 species of marine phytoplankton. *J. Exp. Mar. Biol. Ecol.* **50**: 119–132.
- CULLEN, J. J., AND R. W. EPPLEY. 1981. Chlorophyll maximum layers of the southern California Bight and possible mecha-

- nisms of their formation and maintenance. *Oceanol. Acta* **4**: 23–32.
- DENMAM, K. L., AND A. E. GARGETT. 1983. Time and space scales of vertical mixing and advection of phytoplankton in the upper ocean. *Limnol. Oceanogr.* **28**: 801–815.
- DEWEY, R. K., A. E. GARGETT, AND N. S. OAKEY. 1987. A microstructure instrument for profiling oceanic turbulence in coastal bottom boundary layers. *J. Atmos. Ocean. Tech.* **4**: 288–297.
- EFRON, B., AND G. GONG. 1983. A leisurely look at the bootstrap, the jack-knife and cross-validation. *Am. Stat.* **37**: 36–48.
- FAIRBANKS, R. G., AND P. H. WIEBE. 1980. Foraminifera and chlorophyll maximum: Vertical distribution, seasonal succession, and paleoceanographic significance. *Science* **209**: 1524–1529.
- FERNÁNDEZ, E., J. J. FRITZ, AND W. M. BALCH. 1996. Chemical composition of the coccolithophorid *Emiliania huxleyi* under light-limited steady state growth. *J. Exp. Mar. Biol. Ecol.* **207**: 149–160.
- FINCH, M. S., D. J. HYDES, C. H. CLAYSON, B. WEIGL, J. DAKIN, AND P. GWILLIAM. 1998. A low power ultra violet spectrophotometer for measurement of nitrate in seawater: introduction, calibration, and initial sea trials. *Anal. Chim. Acta* **377**: 167–177.
- GOERING, J. J., D. D. WALLEN, AND R. M. NAUMAN. 1970. Nitrogen uptake by phytoplankton in the discontinuity layer of the eastern subtropical Pacific Ocean. *Limnol. Oceanogr.* **15**: 789–796.
- GRASSHOFF, K. M., K. M. ERHARDT, AND K. KREMLING. 1983. Methods of seawater analysis. Verlag-Chemie.
- HOLLIGAN, P. M., P. J. L. WILLIAMS, D. PURDIE D., AND R. P. HARRIS. 1984. Photosynthesis, respiration and nitrogen supply of plankton populations in stratified, frontal and tidally mixed shelf waters. *Mar. Ecol. Prog. Ser.* **17**: 201–213.
- HORNE, E. P. W., J. W. LODER, C. E. NAMIE, AND N. S. OAKEY. 1996. Turbulence dissipation rates and nitrate supply in the upper water column on Georges Bank. *Deep-Sea Res. II* **43**: 1683–1712.
- JAMART, B. M., D. F. WINTER, K. BANSE, G. C. ANDERSON, AND R. K. LAM. 1977. A theoretical study of phytoplankton growth and nutrient distribution in the Pacific Ocean off the north-western U.S. coast. *Deep-Sea Res.* **24**: 753–773.
- JOINT, I. R., N. J. P. OWENS, AND A. J. POMROY. 1986. Seasonal production of photosynthetic picoplankton and nanoplankton in the Celtic Sea. *Mar. Ecol. Prog. Ser.* **28**: 251–258.
- , AND A. J. POMROY. 1988. Allometric estimation of the productivity of phytoplankton assemblages. *Mar. Ecol. Prog. Ser.* **47**: 161–168.
- LE CORRE, P., AND S. L'HELGUEN. 1993. Nitrogen source for uptake by *Gyrodinium cf. aureolum* in a tidal front. *Limnol. Oceanogr.* **38**: 446–451.
- LEGENDRE, L., S. DEMERS, AND D. LEFAIVRE. 1986. Biological production at marine ergoclines, p. 1–29. *In* J. C. J. Nihoul [ed.], *Marine interfaces ecohydrodynamics*. Elsevier Oceanography Series Vol. 42.
- LEWIS, M. R., W. G. HARRISON, N. S. OAKEY, D. HEBERT, AND T. PLATT. 1986. Vertical nitrate fluxes in the oligotrophic ocean. *Science* **234**: 870–873.
- LORENZEN, C. J. 1966. A method for the continuous measurement of *in vivo* chlorophyll concentration. *Deep-Sea Res.* **13**: 223–227.
- MOUM, J. N. 1996. Efficiency of mixing in the main thermocline. *J. Geophys. Res.* **101**: 12,057–12,069.
- NIMMO SMITH, W. A. M., S. A. THORPE, AND A. GRAHAM. 1999. Surface effects of bottom-generated turbulence in a shallow tidal sea. *Nature* **400**: 251–254.
- OSBORN, T. R. 1980. Estimates of the local rate of vertical diffusion from dissipation measurements. *J. Phys. Oceanogr.* **10**: 83–89.
- PINGREE, R. D., AND L. PENNYCUICK. 1975. Transfer of heat, fresh water and nutrients through the seasonal thermocline. *J. Mar. Biol. Ass. U.K.* **55**: 261–274.
- PLANAS, D., S. AGUSTI, C. M. DUARTE, T. C. GRANATA, AND M. MERINO. 1999. Nitrate uptake and diffusive nitrate supply in the Central Atlantic. *Limnol. Oceanogr.* **44**: 116–126.
- PROBYN, T. A., B. A. MITCHELLNES, AND S. SEARSON. 1995. Primary productivity and nitrogen uptake in the subsurface chlorophyll maximum on the eastern Agulhas Bank, *Cont. Shelf Res.* **15**: 1903–1920.
- REVELANTE, N., AND M. GILMARTIN. 1973. Some observations of the chlorophyll maximum and primary production in the eastern North Pacific. *Internationale Revue der Gesamten Hydrobiologie* **58**: 819–834.
- SATHYENDRANATH, S., T. PLATT, E. P. W. HORNE, W. G. HARRISON, O. ULLOA, R. OUTERBRIDGE, AND N. HOEPPFNER. 1991. Estimation of new production in the ocean by compound remote sensing. *Nature* **353**: 129–133.
- SHARPLEY, J., AND P. TETT. 1994. Modelling the effect of physical variability on the midwater chlorophyll maximum. *J. Mar. Res.* **52**: 219–238.
- SIMPSON, J. H., W. R. CRAWFORD, T. P. RIPPETH, A. R. CAMPBELL, AND J. V. S. CHEOK. 1996. The vertical structure of turbulent dissipation in shelf seas. *J. Phys. Oceanogr.* **26**: 1579–1590.
- , T. P. RIPPETH, AND A. R. CAMPBELL. 2000. The phase lag of turbulent dissipation in tidal flow, p. 57–67. *In* T. Yanagi [ed.], *Interaction between estuaries, coastal seas and shelf seas*. Terra Scientific.
- STEELE, J. H. 1964. A study of production in the Gulf of Mexico. *J. Mar. Res.* **22**: 211–221.
- STEELE, J. H., AND C. S. YENTSCH. 1960. The vertical distribution of chlorophyll. *J. Mar. Biol. Assoc. U.K.* **39**: 217–226.
- STRASS, V. 1990. On the calibration of large-scale fluorometric chlorophyll measurements from towed undulating vehicles. *Deep-Sea Res.* **37**: 525–540.
- TETT, P. B., AND OTHERS. 1993. Biological consequences of tidal stirring gradients in the North Sea. *Philos. Trans. R. Soc. Lond.* **A343**: 493–508.
- VARELA, R. A., A. CRUZADO, J. TINTORÉ, AND E. GARCIA LADONA. 1992. Modelling the deep chlorophyll maximum: A coupled physical-biological approach. *J. Mar. Res.* **50**: 441–463.
- WELSCHMEYER, N. A. 1994. Fluorometric analysis of chlorophyll a in the presence of chlorophyll-b and pheopigments. *Limnol. Oceanogr.* **39**: 1985–1992.

Received: 3 March 2000

Accepted: 16 October 2000

Amended: 8 November 2000